Audio Engineering Society

Conference Paper 11

Presented at the International Conference on Spatial and Immersive Audio
2023 August 23–25, Huddersfield, UK

Robust Binaural Measurements in the Ear Canal Using a Two-Microphone Array

Viktor Gunnarsson[1,2] and Sead Smailagić[2,3]

[1]*Signals and Systems Division, Uppsala University, Sweden*
[2]*Dirac Research AB, Uppsala, Sweden*
[3]*Signaton AB, Helsingborg, Sweden*

Correspondence should be addressed to Viktor Gunnarsson (viktor.gunnarsson@dirac.com)

ABSTRACT

Accurate binaural rendering requires accurate reproduction of binaural signals at the eardrum, which in turn requires adequate binaural technology. We propose a method to measure head-related & headphone transfer functions with a two-microphone array in the ear canal. By implementing a cardioid directional pattern, the forward and reverse propagating sound pressure components are measured separately, thus avoiding the influence of standing waves in the ear canal on the measurements. The method is useful in filter design for individualized binaural rendering that, compared with the blocked-canal method, does not assume acoustically 'open' headphones to be used. The method also mitigates the excessive sensitivity to microphone position of regular open-canal measurements. Validation measurements are conducted using a natural scale replica ear and a MEMS microphone array.

1 Introduction

Headphone-based binaural rendering allows for realistic reproduction of auditory experiences if the reproduced sound pressure at the eardrums matches that of a real sound field or sound source in a certain direction [1–3]. However, accurate reproduction of binaural signals at the eardrums is challenging and requires careful attention to binaural measurement technique and filter design [4]. In principle, an anechoic sound recording can be rendered as a virtual source in direction Ω by convolving it with a filter $H_v(\omega,\Omega)$, unique for each ear, defined as

$$H_v(\omega,\Omega) = \frac{HRTF(\omega,\Omega)}{HpTF(\omega)}. \quad (1)$$

where ω is angular frequency, $HRTF(\omega,\Omega)$ is the Head-Related Transfer-Function (HRTF) that describes the sound transfer function from free-field to a well-defined point in the ear, and $HpTF(\omega)$ is the headphone transfer function to the same point. Both HRTFs and HpTFs vary greatly between individuals [5, 6]. Creating a virtual auditory space with minimum timbral artifacts, correct localization, and full externalization thus generally requires both individual HRTFs [5], and individual HpTFs [7, 8].

A fundamental consideration in binaural technology is the selection of a reference point in the ear where HRTFs and HpTFs are measured. The ear canal can be likened to a tube that is open at one end and closed at the other. Due to its small diameter, around 7.4 mm on

average, wave propagation within the ear canal is often modeled as one-dimensional at audible frequencies. However, the length of the ear canal, around 25 mm on average, is not negligible compared to the wavelength, and a standing wave pattern exists in the ear canal that makes measurements in the ear canal strongly dependent on the exact measurement position. Therefore, HRTFs and HpTFs that are to be combined as in Eq. (1) need to refer to the same reference point.

Hammershøi et. al confirmed that sound transmission to the eardrum from different points in the ear canal is independent of the direction of incidence of sound to the head [9]. They concluded this to be valid over most of the audible spectrum, including from the open or blocked ear canal entrance. An implication of this is that any point in the ear canal can be selected as the reference point when measuring HRTFs and HpTFs while theoretically achieving accurate sound reproduction at the eardrum. Measurements in the ear canal can for example be conducted using a miniature electret or MEMS microphone. In practice, it is often challenging to avoid a small occasional repositioning of the in-ear microphone in between the HRTF and HpTF measurements, for example when taking the headphones on or off, or due to head movements. This leads to inevitable coloration being introduced in the binaural rendering filter of Eq. (1), which will be further elaborated on in section 2.1 of this article.

One choice of reference point is to measure directly at the eardrum, as in e.g. [1]. Probe tube microphones are typically used to avoid damaging the delicate eardrum. In addition to the possible discomfort of such measurements, a complicating factor is that the eardrum position is not defined by a single point along the canal since it terminates the ear canal at an oblique angle. At the highest audible frequencies, the exact probe position at the eardrum has a large effect on the measured response [10].

The most common reference point for HRTF measurements is at the blocked ear canal entrance [11], for several reasons. HRTF measurements at the blocked ear canal are considered to retain full spatial information [12]. Compared to measurements at the open ear canal, the blocked-canal method removes a source of individual variation from HRTF or HpTF measurements that is due to the individual ear canal acoustics, thus making the measurements more suitable for non-individualized reproduction [9, 12]. It is also relatively easy to achieve a stable and well-defined microphone position with the blocked-canal method. However, accurate reproduction of sound pressure at the eardrum with the blocked-canal method generally relies on the assumption that the headphones used have free-air equivalent coupling (FEC) to the ear, i.e., that the headphones are acoustically 'open' and do not significantly affect the acoustic impedance seen from the ear canal. Otherwise, a coloration is introduced corresponding to the so-called pressure-division ratio [6]. The FEC condition is somewhat limiting as most headphones on the market are not fully FEC compatible.

The trade-offs involved with the above-mentioned methods have incited further research into binaural measurement methods. Hiipakka et. al. used a miniature pressure-velocity sensor to measure sound pressure and particle velocity at the entrance of the open ear canal [13, 14]. They proposed a method to estimate the sound pressure at the eardrum based on the acoustic energy density at the ear canal entrance. In an evaluation of the method for individualized binaural synthesis, it performed significantly better than the blocked-canal method both with regards to the measured error in sound pressure at the eardrum [13], and in a listening test on perceived coloration [15]. A factor preventing the adoption of this method, however, is that miniature pressure-velocity sensors suitable for binaural measurements are so far not widely available in the marketplace.

In this article, we propose a two-microphone method suitable for open-canal binaural measurements that can be used with low-cost miniature MEMS microphones. By implementing a cardioid pickup pattern using two closely spaced microphones, the forward (incident) and reverse (reflected) propagating sound waves in the ear canal can be measured separately. Thus, by avoiding the influence of standing-wave patterns on the measurements, the exact microphone location in the ear canal becomes much less critical compared to single-microphone open ear canal measurements, and evaluation of Eq. (1) becomes more robust to small microphone displacements during the measurement session. There is also no requirement for FEC-compatible headphones.

Section 2 presents the proposed method by first analyzing simulations on a simple ear canal model and then presenting the cardioid design equations to measure the forward and reverse pressure waves. Section 3 presents

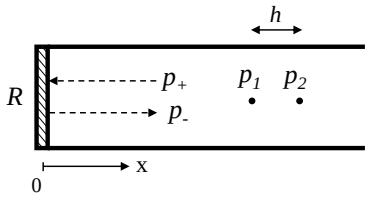

Fig. 1: Model of the ear canal as a one-dimensional transmission line, terminated at $x = 0$ with the eardrum reflectance R.

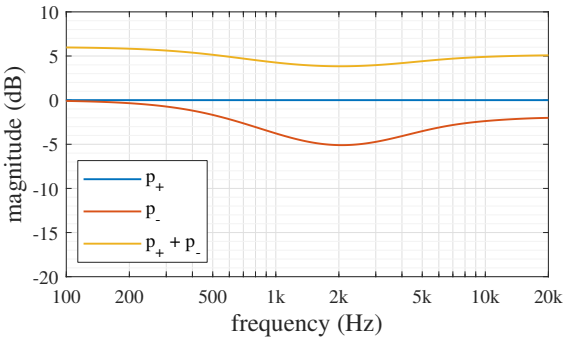

Fig. 2: Modeled magnitude responses of the forward and reverse pressure components in the ear canal model, and their sum at the eardrum position $x = 0$.

a prototype microphone array and validation measurements on a replica ear model, followed by discussion and conclusions.

2 Two-Microphone Measurement Method

2.1 Ear Canal Model

To illustrate the concepts discussed, we employ a simple model of the ear canal as a lossless straight-walled tube with one-dimensional plane wave propagation, illustrated in Figure 1. The tube is terminated at one end by a surface with reflectance factor $R(\omega)$, representing the eardrum. According to the time-harmonic solution to the 1D wave equation in the tube [16], the sound pressure $p(x,\omega)$ along the tube is a sum of a forward-traveling incident wave $p_+(x,\omega)$ and a reverse traveling wave $p_-(x,\omega)$ that has been reflected in the eardrum. In the following we drop the argument ω for conciseness. With the geometry defined by Figure 1, we have

$$p_+(x) = \hat{p}e^{jkx} \tag{2}$$

$$p_-(x) = \hat{p}Re^{-jkx} \tag{3}$$

$$p(x) = p_+(x) + p_-(x), \tag{4}$$

where $\hat{p}$ is the peak sound pressure of the incident wave, $k = \omega/c$, c is the speed of sound and $j = \sqrt{-1}$.

The reflectance factor R in the tube model can be determined from sound pressure measurements at two points along the tube, as described by the standardized two-microphone method for determining acoustic properties of material samples in an impedance tube [17]. The eardrum reflectance for real ears is highly variable between individuals. For the simulations in this section we use a model for R that was fit approximately to average data published in [18].

With the frequency response of the incident wave designated as being flat ($\hat{p} = 1$), Figure 2 illustrates the magnitude of the sound pressure components of Eqs. (2)-(4), at the eardrum position ($x = 0$). For this case, the magnitude of the reflectance factor R equals the magnitude of $p_-(x)$, and can thus be read out of the figure as well.

Figure 3(a) illustrates the strong dependency on measurement position when measuring the total sound pressure in the ear canal. The graph shows the simulated sound pressure response at different points along the ear canal model, normalized to the pressure at the eardrum position. The interaction between the forward and reverse pressure waves creates a standing-wave pattern in the ear canal, resulting in a magnitude response that varies strongly with position.

A small displacement of the microphone can occur between subsequent measurements of HRTFs and HpTFs, leading to coloration when evaluating Eq. (1) to design a filter for binaural synthesis. The introduced coloration corresponds to the magnitude response difference between the two slightly different positions along the ear canal. Figure 3(b) shows the simulated coloration resulting from a microphone displacement of 1 mm at different original measurement points along the ear canal. As can be seen, the coloration is substantial at high frequencies.

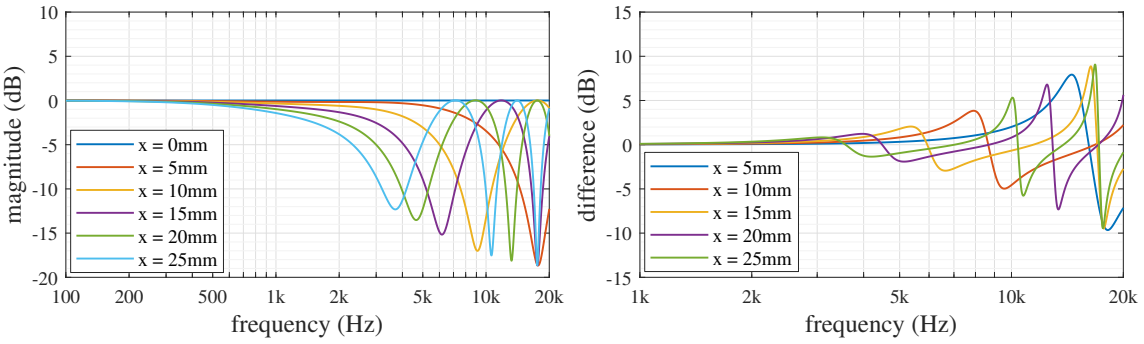

(a) **(b)**

Fig. 3: a) Simulated sound pressure magnitude response at different points along the ear canal (normalized to the eardrum pressure), and **b)** relative change in magnitude response for a microphone displacement of 1 mm.

The modeled magnitude responses of the forward and reverse pressure waves, on the other hand, are not affected by standing waves and are identical for different points along the tube model. This observation motivates measurement of these pressure components instead of the total sound pressure in the ear canal, for use in filter design for individual binaural synthesis. The proposed measurement method is outlined in the following.

2.2 Cardioid Array Design

The forward and reverse pressure responses can be determined from sound pressure measurements at two points $p_1 = p(x_1)$ and $p_2 = p(x_2)$ along the tube. The points are illustrated in Figure 1. Using Eqs. (2)-(4), a relationship between the forward and reverse pressure and the measurements p_1 and p_2 can be defined as

$$\begin{bmatrix} 1 & e^{jkh} \\ e^{jkh} & 1 \end{bmatrix} \begin{bmatrix} p_+(x_1) \\ p_-(x_2) \end{bmatrix} = \begin{bmatrix} p_1 \\ p_2 \end{bmatrix}. \tag{5}$$

Here, $h = x_2 - x_1$ denotes the spacing between the measurement points. Solving for the forward and reverse pressure gives

$$\begin{bmatrix} p_+(x_1) \\ p_-(x_2) \end{bmatrix} = \frac{1}{1-e^{jk2h}} \begin{bmatrix} 1 & -e^{jkh} \\ -e^{jkh} & 1 \end{bmatrix} \begin{bmatrix} p_1 \\ p_2 \end{bmatrix}. \tag{6}$$

The above expression can be written more compactly in terms of filters H_1 and H_2, obtaining

$$\begin{bmatrix} p_+(x_1) \\ p_-(x_2) \end{bmatrix} = \begin{bmatrix} H_1 & H_2 \\ H_2 & H_1 \end{bmatrix} \begin{bmatrix} p_1 \\ p_2 \end{bmatrix} \tag{7}$$

where, after some algebraic simplifications, H_1 and H_2 are given by

$$\begin{aligned} H_1 &= \frac{1}{1-e^{jk2h}} = \frac{-e^{-jkh}}{e^{jkh}-e^{-jkh}} = \frac{-e^{-jkh}}{2j\sin kh}, \\ H_2 &= \frac{-e^{jkh}}{1-e^{jk2h}} = \frac{1}{e^{jkh}-e^{-jkh}} = \frac{1}{2j\sin kh}. \end{aligned} \tag{8}$$

The forward and reverse pressures, $p_+(x_1)$ and $p_-(x_2)$, are calculated by filtering the measurements, p_1 and p_2, using the filters H_1 and H_2. A closer examination reveals that H_1 and H_2 are identical to standard expressions used for implementing a directional pickup pattern on a two-microphone array that approaches a cardioid in the free field [19]. This is logical since an ideal cardioid pattern has unity gain on its frontal axis and zero gain in the opposite direction. Therefore, depending on the orientation of the cardioid in the ear canal, either $p_+(x_1)$ or $p_-(x_2)$ is measured.

The spacing h between the microphones must not be selected too large. The common denominator of H_1 and H_2 becomes undefined if $\sin(kh) = 0$, or equivalently if h equals a multiple of half a wavelength. When working with discrete-time signals, this leads to a practical upper limit of $h < c/f_s$, where f_s is the sample rate. At 48 kHz sample rate the limit is around $d < 7.2$ mm.

The filter gain of H_1 and H_2 is approximately proportional to $1/\omega h$ and can become very large at low frequencies when h is small. Large filter gain can cause issues with signal-to-noise ratio and excessive sensitivity to the precise gain matching between the microphones. It is therefore not suitable to implement H_1

and H_2 directly. To address the gain problem, we transition the cardioid to an omnidirectional response at low frequencies. For this, we use zero-phase low-pass and high-pass crossover filter functions H_{lp} and H_{hp} defined as

$$\begin{aligned} H_{lp} &= \frac{1}{1+(\omega/\omega_c)^N}, \\ H_{hp} &= 1 - H_{lp}. \end{aligned} \tag{9}$$

Here, ω_c is the crossover frequency, and N is the filter order. As shown in Figure 3(a), the sound pressure becomes homogeneous in the ear canal at lower frequencies. The pressure components $p_+(x)$ and $p_-(x)$ are thus essentially in phase at lower frequencies and can be approximated as $p_+(x) \approx p_-(x) \approx p(x)/2 \approx (p_1 + p_2)/4$. We obtain the final filters by applying the cardioid filter in the high-pass branch and a scaled sum of the microphone signals in the low-pass branch. This gives modified filters that approximately satisfy Eq. (7):

$$\begin{aligned} H_1^{'} &= H_{lp}/4 + H_{hp}H_1 \\ H_2^{'} &= H_{lp}/4 + H_{hp}H_2. \end{aligned} \tag{10}$$

This modification helps to mitigate the gain problem at low frequencies, while allowing estimation of $p_+(x)$ and $p_-(x)$ over the full frequency range.

3 Validation Measurements

Validation measurements were performed on a replica ear using a prototype microphone array consisting of two miniature MEMS microphones. The purpose of the measurements was twofold: to confirm that measured estimates of the forward and reverse pressures, $p_+(x)$ and $p_-(x)$, are not affected by standing wave notches and depend less on position than the total sound pressure; and to test the utility of cardioid measurements in filter design for binaural rendering. The replica ear is made out of transparent rubber and has been cast from a real person. It has a realistically shaped ear canal that measures approximately 28 mm in length.

Figure 4(a) shows a picture of the replica ear and the microphone array together with cabling and connectors, and Figure 4(b) shows a closer view of the MEMS microphone capsules. The capsule model is CUI Devices CMM-2718AT-3817NC-TR, chosen due to its small footprint and adequate SNR. It is an analog, top port design. Two capsules have been glued together to form an

(a)

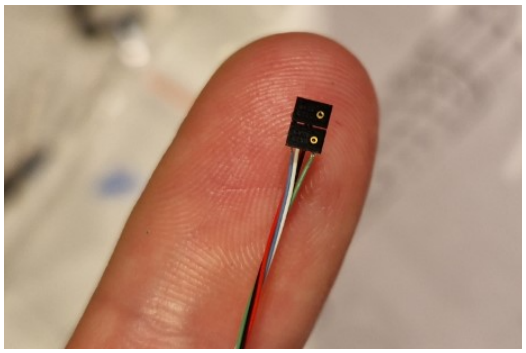

(b)

Fig. 4: a) Replica ear and microphone array used for validation measurements., **b)** Close-up view of MEMS microphone array capsules.

array with a spacing of $h = 2.2$ mm between the ports. The cabling uses thin 36 AWG wire and the MEMS soldering area has been coated with an epoxy layer to increase durability and prevent electric short-circuiting. The total package measures 3.9x2.8x1.5 mm. The microphone array is connected to a sound card using two XLR connectors, and a custom-designed PCB inside the XLR connectors allows the microphones to be 48V phantom powered from the sound card.

Cardioid filters were designed for the microphone array according to Eqs. (8)-(10), using a crossover between omnidirectional and cardioid response of order $N = 8$

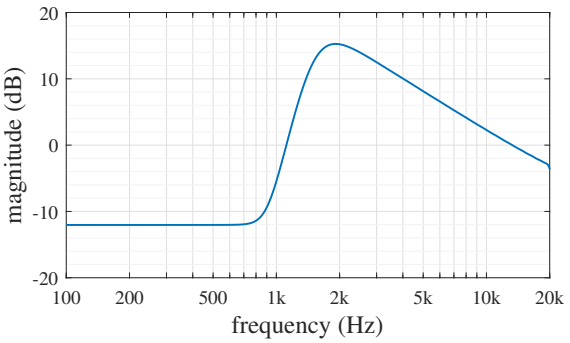

Fig. 5: Magnitude response of filters $H_1^{'}$ and $H_2^{'}$ for the prototype cardioid array.

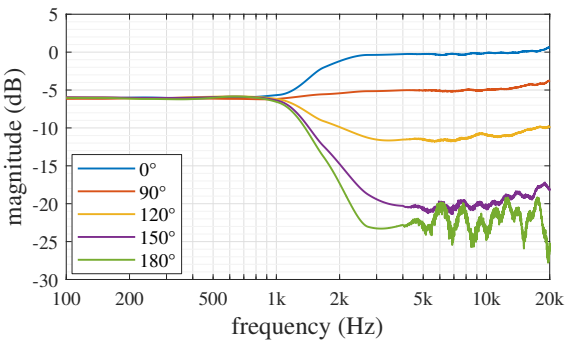

Fig. 6: Measured polar response of the prototype cardioid array.

and with crossover frequency 1.5 kHz. Figure 5 displays the resulting filter magnitude response. The filters were realized as time-domain finite impulse response (FIR) filters by taking the inverse FFT[1].

The microphone capsules were calibrated to differ in gain by less than ± 0.1 dB. Figure 6 shows a measurement of the resulting free-field polar response of the microphone array. As expected, the array becomes omnidirectional below the crossover frequency and approaches a unidirectional response at high frequencies. In line with the reasoning in section 2.2, the free-field array response is down 6 dB at low frequencies to compensate for the array responding to only "half" the sound pressure in the ear canal above the crossover frequency (p_+ or p_-) but the total sound pressure ($p_+ + p_-$) below it.

In section 3.1 below we compare cardioid array and single microphone measurements at different points in the ear canal of the replica ear. Then, in section 3.2, we investigate the error in reproduced sound pressure at the eardrum position of the replica ear, when headphones are used to reproduce a measured binaural room impulse response (BRIR).

3.1 Measurements at Different Ear Canal Positions

The pressure components $p_+(x)$, $p_-(x)$, and total sound pressure $p_1(x)$ were measured at 5 mm intervals in the ear canal of the replica ear. For these measurements, the replica ear was placed at the edge of a table in a normally reflective room, and impulse responses were measured from a Genelec 8341-series coaxial speaker to the microphone array in the ear canal. The speaker was placed at a distance of 70 cm and at a similar height as the ear, and at an azimuth angle of 45° from the frontal axis of the ear. A logarithmic sine sweep was used as measurement signal, and the captured impulse responses were windowed to 4 ms length to simulate free-field conditions[2].

The sound field pressure components were estimated according to Eq. (7). The resulting magnitude responses, with 1/8-octave smoothing applied, are presented in Figure 7. Figure 7(a) shows the measured response of the total sound pressure $p_1(x)$, normalized by the "eardrum" sound pressure $p_1(0)$. The impact of standing waves on $p_1(x)$ is large, as predicted by the simulation in Figure 3. The notches are deeper than in the simulation because the reflectance at the termination of the replica ear canal is higher than in an average real ear.

Figures 7(b) and 7(c) show the measured estimates of $p_+(x)$ and $p_-(x)$, respectively, again normalized by $p_1(0)$. Effects of standing waves are much reduced in the measured $p_+(x)$ and $p_-(x)$ and the spread between the curves for the different measurement positions is much smaller than for the total pressure $p_1(0)$. The measurements of $p_+(x)$ and $p_-(x)$ at the outermost position at 25 mm from the eardrum have somewhat more

[1] after adding a suitable modeling delay and a windowed-sinc low-pass filter near the Nyquist frequency to the filter equations.

[2] The loss of low-frequency information due to windowing has a negligible impact on the following analysis which only considers relative spectral differences.

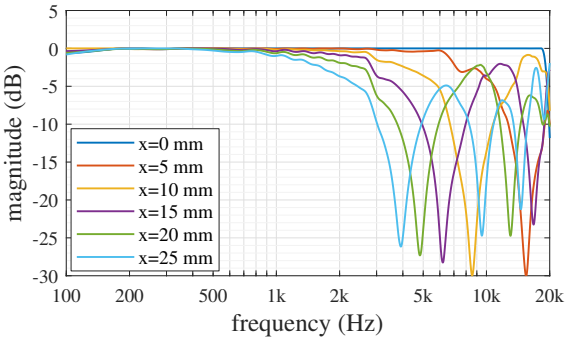

(a) $p_1(x)/p_1(0)$

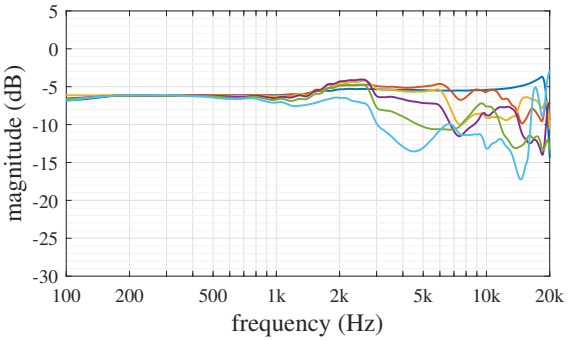

(b) $p_+(x)/p_1(0)$

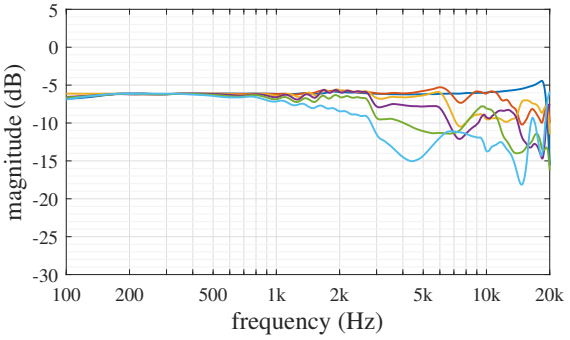

(c) $p_-(x)/p_1(0)$

Fig. 7: a) Measured sound pressure $p_1(x)$ at different points in the ear canal of the replica ear, **b)** Measured forward pressure $p_+(x)$, **c)** Measured reverse pressure $p_-(x)$. All curves are normalized by the pressure response $p_1(0)$ at the eardrum reference position.

magnitude response ripple than for the other positions. In practice, measurement positions past the first bend of the ear canal may be preferable to measurements at the ear canal entrance.

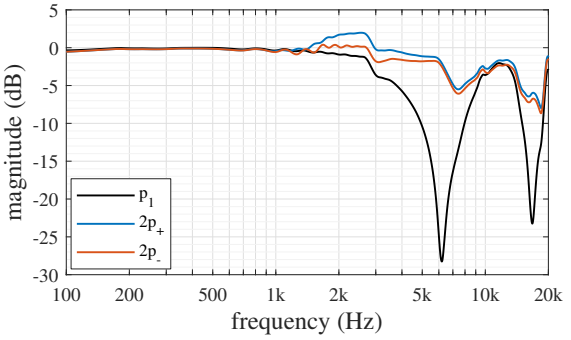

Fig. 8: Measured magnitude response of sound pressure components at 15 mm from the eardrum position, normalized by the pressure response $p_1(0)$ at the eardrum position.

3.1.1 Comments on Measurements

In the transmission-line ear canal model discussed in section 2.1, the forward and reverse pressure magnitude response is independent of position. A real ear canal has a varying cross-sectional area along its length and tapers off toward the eardrum, and can be more accurately modeled as an acoustic horn [20]. The measured responses in Figure 7 tend to fall off at high frequencies for measurement positions farther away from the eardrum position, which is consistent with published results on the spatial distribution of sound pressure in the human ear canal [20].

Figure 8 shows a comparison between the measured total, forward, and reverse pressure magnitude responses 15 mm from the eardrum position using the same data as in Figure 7. The standing wave notches are largely absent from the forward and reverse pressure responses. Some remaining ripple in the measured $p_+(x)$ and $p_-(x)$ might be related to an imperfect separation of the forward and reverse pressure waves due to, for example, imperfect microphone calibration. Also, the response of the cardioid microphone array depends on its alignment with the length axis of the ear canal, which is difficult to control exactly.

3.2 Error in Reproduced Sound Pressure at the Eardrum

A second series of measurements were performed to verify the use of cardioid array measurements in fil-

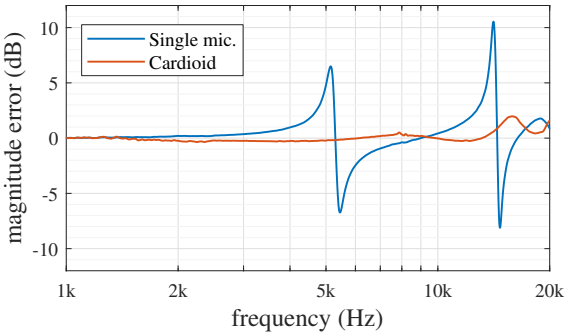

Fig. 9: Magnitude response error in reproduced sound pressure at the eardrum position of the replica ear, in example filter design for binaural rendering. Comparison between filters based on cardioid and single microphone measurements.

ter design for binaural rendering. The replica ear was mounted in a jig made out of medium-density fiberboard that allowed a pair of headphones to be placed over it. A third miniature MEMS microphone was placed at the eardrum position of the replica ear and the two-microphone array was placed at around 18 mm from the eardrum position.

A BRIR was measured simultaneously with the three microphones, with the Genelec speaker at around 50 cm distance. After the BRIR measurement, the two-microphone array was intentionally moved around 1 mm outward in the ear canal. Next, a pair of Sennheiser HD600 headphones was put over the ear, and the headphone response (HpTF) was measured with the three microphones. This allowed the design of a filter for headphone rendering of the BRIR according to Eq. (1), by replacing the HRTF in the numerator with the frequency-domain equivalent of the measured BRIR, i.e., the measured binaural room transfer function (BRTF).

Three filters were designed: one based on the BRTF and HpTF measured at the eardrum position, designated as the reference filter (H_v^{ref}); a second filter, H_v^c, based on the cardioid measurements; and a third filter, H_v^m, using measurements by the single inner microphone in the two-microphone array. To assess the reproduction error at the eardrum when using H_v^c and H_v^m for binaural rendering, we calculated H_v^c/H_v^{ref} and H_v^m/H_v^{ref}, respectively. Figure 9 displays the reproduction error for the two filters.

Figure 9 shows that the shift in microphone position between the BRTF and HpTF measurement resulted in large coloration with sharp magnitude response peaks in the filter based on single microphone measurements. In contrast, the filter based on cardioid measurements reproduces sound pressure at the eardrum position with high accuracy. In a real ear, the single microphone case would likely exhibit somewhat lower but still significant coloration due to lower eardrum reflectance than that of the replica ear, c.f. Figure 3(b).

4 Discussion

The validation measurements in the previous section suggest that measurements of $p_+(x)$ or $p_-(x)$ are suitable for use in filter design problems for binaural synthesis, due to their relative insensitivity to variation in the measurement position. The absence of standing wave notches in the measurements can also make inverse filter design for headphone correction better conditioned. The forward pressure $p_+(x)$ typically has a slightly higher level than the reflected reverse pressure $p_-(x)$, and may therefore be preferred from an SNR perspective.

The forward pressure level has previously been suggested for use e.g. in connection with the fitting of hearing aids, to avoid the influence of standing waves on measurements in the ear canal [10]. A conventional procedure for calculating the forward pressure is model-based and relies on a single sound pressure measurement in the ear canal with an earphone probe, together with knowledge of the Thévenin-equivalent acoustic impedance and pressure of the sound source. A benefit of the method presented here is that it does not require estimation of any model parameters and can be used both for free-field measurements and with headphones of different types.

There are several methods that could be used to estimate sound pressure at the eardrum from the two-microphone measurement. One is to sum $p_+(x)$ and $p_-(x)$ with appropriate time alignment. The energy-based method of Hiipakka et. al. can also be an alternative [13], seeing that acoustic particle velocity can be estimated from two closely spaced microphones [16]. However, this topic is left for future research.

The proposed two-microphone method naturally adds some additional complexity over traditional single-microphone binaural measurements. Further research is needed to demonstrate the practicality of the proposed method for measurements on real ears and to investigate practical filter design cases for binaural rendering. Sensitivity to microphone calibration mismatch and its effect on the measurements should also be investigated.

5 Summary

A method for measuring the forward and reverse pressure components with a cardioid microphone array in the ear canal was presented. The technique is suitable to use for measuring HRTFs and HpTFs with an open ear canal. Compared to the blocked-canal method, open ear canal measurements are useful for designing filters for binaural rendering that do not require headphones with special FEC properties.

Validation measurements in a replica ear confirm that the measured forward and reverse pressures are largely unaffected by standing wave notches and show much less positional dependence than the total pressure in the ear canal. This indicates that the proposed measurement technique is more robust to accidental variations in the microphone position during the measurements, which implies lower error and higher fidelity in filter design for binaural rendering.

References

[1] Wightman, F. L. and Kistler, D. J., "Headphone simulation of free-field listening. I: Stimulus synthesis," *The Journal of the Acoustical Society of America*, 85(2), pp. 858–867, 1989, doi: 10.1121/1.397557.

[2] Brinkmann, F., Lindau, A., and Weinzierl, S., "On the authenticity of individual dynamic binaural synthesis," *The Journal of the Acoustical Society of America*, 142(4), pp. 1784–1795, 2017, doi: 10.1121/1.5005606.

[3] Griesinger, D., "Laboratory Reproduction of Binaural Concert Hall Measurements through Individual Headphone Equalization at the Eardrum," in *142nd Convention of the Audio Engineering Society*, 2017.

[4] Møller, H., "Fundamentals of binaural technology," *Applied Acoustics*, 36, pp. 171–218, 1992.

[5] Møller, H., Sørensen, M., Jensen, C., and Hammershøi, D., "Binaural technique: Do we need individual recordings?" *The Journal of the Audio Engineering Society*, 44(6), pp. 451–464, 1996.

[6] Møller, H., Hammershøi, D., Jensen, C. B., and Sørensen, M. F., "Transfer Characteristics of Headphones Measured on Human Ears," *Journal of the Audio Engineering Society*, 43(4), pp. 203–217, 1995.

[7] Pralong, D. and Carlile, S., "The role of individualized headphone calibration for the generation of high fidelity virtual auditory space," *The Journal of the Acoustical Society of America*, 100(6), pp. 3785–3793, 1996, doi:10.1121/1.417337.

[8] Engel, I., Alon, D. L., Robinson, P. W., and Mehra, R., "The Effect of Generic Headphone Compensation on Binaural Renderings," in *AES International Conference on Immersive and Interactive Audio*, 2019.

[9] Hammershøi, D. and Møller, H., "Sound transmission to and within the human ear canal," *The Journal of the Acoustical Society of America*, 100(1), pp. 408–427, 1996, doi:10.1121/1.415856.

[10] McCreery, R. W., Pittman, A., Lewis, J., Neely, S. T., and Stelmachowicz, P. G., "Use of forward pressure level to minimize the influence of acoustic standing waves during probe-microphone hearing-aid verification," *The Journal of the Acoustical Society of America*, 126(1), pp. 15–24, 2009, doi:10.1121/1.3143142.

[11] Li, S. and Peissig, J., "Measurement of Head-Related Transfer Functions: A Review," *Applied Sciences*, 10(14), pp. 1–40, 2020, doi:10.3390/app10145014.

[12] Møller, H., Sørensen, M. F., Hammershøi, D., and Jensen, C. B., "Head-Related Transfer Functions of Human Subjects," *Journal of the Audio Engineering Society*, 43(5), pp. 300–321, 1995.

[13] Hiipakka, M., Kinnari, T., and Pulkki, V., "Estimating head-related transfer functions of human subjects from pressure–velocity measurements," *The Journal of the Acoustical Society of America*, 131(5), pp. 4051–4061, 2012, doi: 10.1121/1.3699230.

[14] de Bree, H.-E., "An Overview of Microflown Technologies," *Acta Acustica united with Acustica*, 89, pp. 163–172, 2003.

[15] Takanen, M., Hiipakka, M., and Pulkki, V., "Audibility of Coloration Artifacts in HRTF Filter Designs," in *AES 45th International Conference: Applications of Time-Frequency Processing in Audio*, 2012.

[16] Blackstock, D. T., *Fundamentals of physical acoustics*, Wiley, New York, 2000, ISBN 978-0-471-31979-5.

[17] ISO-10534-2:1998, *Acoustics — Determination of sound absorption coefficient and impedance in impedance tubes — Part 2: Transfer-function method*, International Organization for Standardization, Geneva, Switzerland, 1998.

[18] Nørgaard, K. M., Fernandez-Grande, E., Schmuck, C., and Laugesen, S., "Reproducing ear-canal reflectance using two measurement techniques in adult ears," *The Journal of the Acoustical Society of America*, 147(4), pp. 2334–2344, 2020, doi:10.1121/10.0001094.

[19] Olson, H. F., "Gradient Microphones," *The Journal of the Acoustical Society of America*, 17(3), pp. 192–198, 1946, doi:10.1121/1.1916315.

[20] Stinson, M. R. and Daigle, G. A., "Comparison of an analytic horn equation approach and a boundary element method for the calculation of sound fields in the human ear canal," *The Journal of the Acoustical Society of America*, 118(4), pp. 2405–2411, 2005, doi:10.1121/1.2005947.